Int J Adv Manuf Technol (2016) 87:1597–1607
DOI 10.1007/s00170-016-8558-8

ORIGINAL ARTICLE

Tolerance analysis and allocation of special machine tool for manufacturing globoidal cams

Yueming Zhang [1] · **Shuting Ji** [1] · **Jing Zhao** [1] · **Lijun Xiang** [2]

Received: 26 October 2015 / Accepted: 26 February 2016 / Published online: 9 March 2016

Abstract In order to produce a special machine tool for manufacturing high-quality globoidal cams, this paper presents a systematic approach for tolerance analysis and tolerance allocation for the special machine tool. Based on the differential geometry and conjugate theory, the machined surface and the surface deviation of a globoidal cam are derived with the help of a VS software. The sensitivity model and the worst-case method are applied to analyze the effects of machine tool errors on the machined surface deviation. Manufacture easiness index which can evaluate the level of manufacture difficulty and can also indirectly imply manufacture cost is proposed. Then, the optimization problems are formulated to the maximize manufacture easiness index subject to quality target of cam surface and manufacture constraints. The optimization results are obtained by using MATLAB implementation of linear programming. To confirm the optimization results, they are applied as a guideline to design and manufacture this special machine tool. After that, a globoidal cam is manufactured on this machine tool and measured on a coordinate measuring machine (CMM). The measuring results demonstrate the effectiveness of the proposed approach.

✉ Shuting Ji
yuncaishu123@163.com

Yueming Zhang
zhangym@bjut.edu.cn

Jing Zhao
zhaojing@bjut.edu.cn

Lijun Xiang
xianglijun@byjc.com.cn

[1] College of Mechanical Engineering and Applied Electronics Technology, Beijing University of Technology, 100 Ping Le Yuan, Beijing, Chaoyang District 100124, People's Republic of China

[2] Beijing No.1 Machine Tool Plant, 16 Shuang He Street, Lin He Industrial Development Zone, Beijing, Shunyi District 101300, People's Republic of China

Keywords Tolerance allocation · Tolerance analysis · Machine tool · Globoidal cam · Surface deviation

1 Introduction

Globoidal cam, the key part of an automatic tool changer, has the features of high indexing precision, compact construction, strong bearing capability, and so on. The surface deviation of the globoidal cam may seriously affect the output accuracy and dynamic performance, such as increasing the tendency of noise and wear. As the globoidal cam is a complex part, the special machine tool is always needed for manufacture. In order to produce the high-quality globoidal cams, the optimal tolerance design for the special CNC machine tool for manufacturing globoidal cams is an important issue.

Computer-aided tolerance design for the special machine tool is a key technology of CAD/CAM. Generally speaking, tolerance allocation (design) consists of three parts: establishment of the relationship between the element tolerance and the final product quality (machined surface deviation), tolerance analysis, and tolerance allocation. The derivation of the globoidal cam surface has been presented by a number of researches. Yan and Chen [1] derived the surface geometry of the globoidal cam by using the conjugate theory. Backhouse and Jones [2] applied the envelope theory to the surface geometry of the globoidal cam. Ji et al. [3] used the offset surface method to derive the globoidal cam surfaces. However, few studies deal with the mathematical problem of the machined cam surface which considers different kinds of machine tool errors.

The tolerance studies about cams mainly focused on the output errors of cam mechanisms. Tsay and Ho [4] identified the analytical expressions for the indexing accuracy of globoidal cam mechanism by considering the manufacturing variables involved in the machining and assembly processes. Cheng [5] proposed an organized process for the transmission error analysis and tolerance synthesis for globoidal cam mechanisms. Wang et al. [6] studied the optimal design of spatial cam mechanism by considering the influences of mechanical errors on output functions and contact conditions. Chang and Wu [7] presented mathematical tools for tolerance analysis and synthesis of cam-modulated linkages. According to the studies mentioned above, the optimal tolerance design for the special machine tool for manufacturing globoidal cams has not been given attention.

It is an essential procedure to analyze the influence of the element errors on the final product quality before the tolerance allocation. A number of tolerance accumulation models are available, and they are classified into two groups: worst-case (WC) models and statistical models [8]. The WC tolerance accumulation model [9, 10] is based on the worst-case situation that all the element deviations reached their extreme limits simultaneously. The root sum of square method (RSS) is the commonly used method in statistical tolerance accumulation. Zhu et al. [11] proposed a new C-NPS method for tolerance analysis, which combines the convex method and non-probabilistic set theory (NPS). Schleich and Wartzack [12] provided a further step toward a computer-aided tolerancing theory by employing skin model shapes in discrete geometry. The review of different tolerance analysis methods have been published in many literatures [13–18].

Determining optimal tolerance involves a trade-off between the level of quality based on functional performance and the costs associated with the tolerance [19]. Thus, the least cost method [20–24] has been the main criterion for tolerance allocation. Other criteria for tolerance allocation include equal tolerance, equal precision, and product robustness design [25]. Singh et al. [26] has discussed details of research carried out and theories developed over the decades on different aspects of tolerance synthesis. In reality, different components have different cost-tolerance relationship. In addition, the published references for the relationship are insufficient and out of date. Thus, it is very difficult to obtain the empirical data for the cost-tolerance relationship. Thus, some researchers tried to find a new objective function for tolerance allocation. Wang et al. [27] used the manufacturing difficulty coefficient which evaluated by the fuzzy-set weight-center method as the criterion for tolerance allocation. Chang and Wu [7] modeled the manufacturability and the assembility as the objective for tolerance allocation.

Henceforth, up to the present, less literature presented systematic approaches for tolerance analysis and synthesis of special machine tool for manufacturing globoidal cams. Based on the conjugate theory and differential geometry, the machined surface of the globoidal cam by considering rotational angle errors, linear offset errors, and the squareness errors of the machine tool is derived. Furthermore, the influence of the machine tool errors on the surface error of the machined globoidal cam are systematically derived and analyzed. Owing to the insufficient empirical data of the cost-tolerance relationship, the concept of the manufacture easiness index which can evaluate the manufacture easiness as well as manufacture cost is proposed. The worst-case accumulation model is chosen for tolerance accumulation. In addition, the optimization model for tolerance synthesis is established by combining with the final product requirements, manufacturing constraints, and the restrictions. With the help of the VS software and MATLAB Optimization Toolbox, the optimal results of tolerance design for the special machine tool of globoidal cams is obtained. In order to validate the effectiveness of the proposed approach, the optimal tolerance results are used as the guideline for manufacturing the special machine tool. After that, a globoidal cam machined by this special machined tool is measured by a CMM.

2 Mathematical model including machine tool errors

2.1 Machine tool configuration

The globoidal cam mechanism is shown in Fig. 1. The turret is driven by the globoidal cam surface to transmit an intermittent motion with periodic variable speed. Analogous to the transmission relationship between the globiodal cam and the turret roller, the configuration of four-axis special machine tool for manufacturing globoidal cams is designed (see Fig. 2).

As shown in Fig. 2, the machine tool consists of two coordinated rotary axes and two slide motion axes, which are noted by A, B and W, Z in order. The generating method is applied

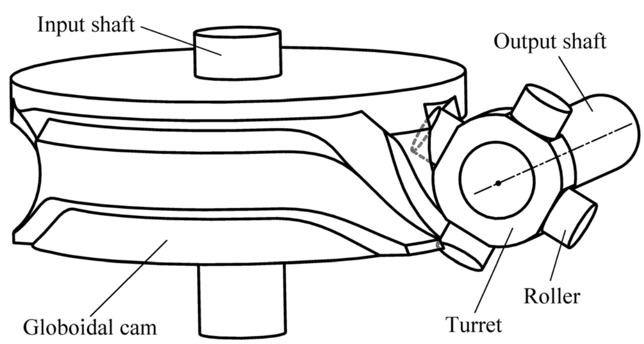

Fig. 1 The globoidal cam mechanism

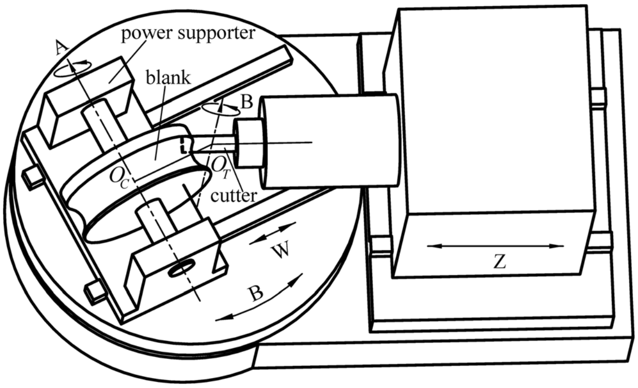

Fig. 2 The configuration of 4-axis special machine tool for manufacturing globoidal cam

to manufacture the globoidal cam. Hence, the dimension of the cutter is equal to the meshing element, and the cutter follows the same path as that of the meshing rollers relative to the cam. In the machining process, the cam blank rotates about *A*-axis, and swivels around *B*-axis (which corresponds to rotary motion of roller around turret axis). *A*-axis and *B*-axis are mutually perpendicular and are equivalent to the input axis and the output axis of the globoidal cam mechanism in Fig. 1, respectively. *W*-axis is used to adjust the distance between *A*-axis and *B*-axis, which is equivalent to the center distance of the globoidal cam mechanism. *Z*-axis is used to adjust the milling depth of the cutter.

2.2 Machine tool errors to be identified

For the configuration shown in Fig. 2, 8 machine tool errors are selected to be identified, including 2 rotational errors, 3 squareness errors, and 3 linear offset errors. The 8 element errors are listed in Table 1 and are delineated in Fig. 3.

2.3 Machined globoidal cam surface considering machine tool errors

The coordinate systems of the special machine tool that contain and not contain machine tool errors are shown in Figs. 3 and 4, respectively. The coordinate system $O_TX_TY_TZ_T$ is fixed to the rotation table of the machine tool. Thus, the Y_T -axis aligns with the *B*-axis of the machine tool, and the angular position of the *B*-axis is β. The coordinate system $O_CX_CY_CZ_C$ is connected to the cam blank, and the rotational angle of the cam blank is α. Thus, the *A*-axis and *B*-axis are coordinated with the relationship $\beta(\alpha)$. If the squareness errors $\Delta\gamma_X$ and $\Delta\gamma_Y$ between the power supporter and the rotation table are omitted, the coordinate system $O_SX_SY_SZ_S$ is attached to the power supporter. The Z_S-axis is coaxial with cam rotation axis Z_C. The X_S-axis is along the perpendicular between Z_S-axis and Y_T-axis, and the center distance between them is a. When the two squareness errors $\Delta\gamma_X$ and $\Delta\gamma_Y$ are taken into account, the real coordinate system fixed to the power supporter is $O_RX_RY_RZ_R$. In other words, Z_R-axis is the real rotation axis of the cam blank. Thus, $O_RX_RY_RZ_R$ is the original rotation position of the cam blank. The distance from a point P on the cutter axis to *B*-axis is b.

The position vector $\boldsymbol{r}_T$ of P in the coordinate system $O_TX_TY_TZ_T$ is as follows:

$$\begin{aligned}\boldsymbol{r}_T &= \begin{bmatrix} 1 & 0 & 0 \\ 0 & \cos(\Delta\delta_x) & \sin(\Delta\delta_x) \\ 0 & -\sin(\Delta\delta_x) & \cos(\Delta\delta_x) \end{bmatrix} \begin{bmatrix} \Delta x \\ \Delta y \\ -b \end{bmatrix} \\ &= \begin{bmatrix} \Delta x \\ \Delta y\cos(\Delta\delta_x) - b\sin(\Delta\delta_x) \\ -\Delta y\sin(\Delta\delta_x) - b\cos(\Delta\delta_x) \end{bmatrix}\end{aligned} \tag{1}$$

The position vector $\boldsymbol{r}_S$ of P in the coordinate system $O_SX_SY_SZ_S$ which is fixed to the ideal position of power supporter is as follows:

$$\begin{aligned}\boldsymbol{r}_S &= \begin{bmatrix} \sin(\beta+\Delta\beta) & 0 & \cos(\beta+\Delta\beta) \\ 0 & -1 & 0 \\ \cos(\beta+\Delta\beta) & 0 & -\sin(\beta+\Delta\beta) \end{bmatrix} \boldsymbol{r}_T + \begin{bmatrix} a+\Delta a \\ 0 \\ 0 \end{bmatrix} \\ &= \begin{bmatrix} -(\Delta y\sin(\Delta\delta_x) + b\cos(\Delta\delta_x))\cos(\beta+\Delta\beta) \\ +\Delta x\sin(\beta+\Delta\beta) + a + \Delta a \\ -(\Delta y\cos(\Delta\delta_x) - b\sin(\Delta\delta_x)) \\ (\Delta y\sin(\Delta\delta_x) + b\cos(\Delta\delta_x))\sin(\beta+\Delta\beta) \\ +\Delta x\cos(\beta+\Delta\beta) \end{bmatrix} = \begin{bmatrix} X_S \\ Y_S \\ Z_S \end{bmatrix}\end{aligned} \tag{2}$$

The position vector $\boldsymbol{r}_R$ of P in the coordinate system $O_RX_RY_RZ_R$ (fixed to the real position of the power supporter

Table 1 Selected machine tool errors

Symbol	Description
$\Delta\alpha$	Rotational error of *A*-axis
$\Delta\gamma_X$	Squareness error of *A*-axis around X_S-axis
$\Delta\gamma_Y$	Squareness error of *A*-axis around Y_S-axis
$\Delta\beta$	Rotational error of *B*-axis
$\Delta\delta_X$	Squareness error of *B*-axis around X_T-axis
Δx	Linear offset error of spindle in *X*-direction
Δy	Linear offset error of spindle in *Y*-direction
Δa	Linear error of *W*-axis

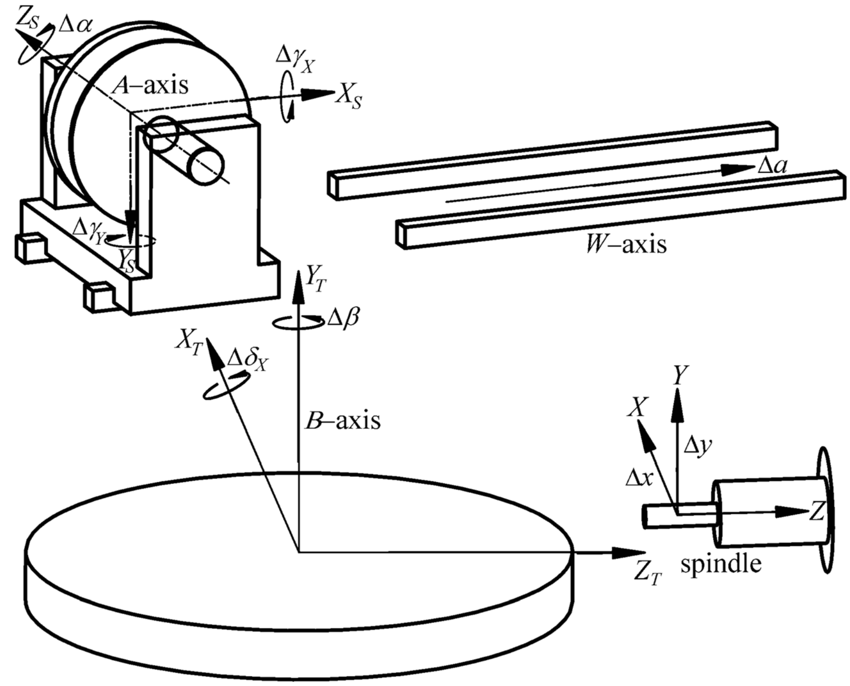

Fig. 3 Machine tool errors considered in this paper

or the original rotation position of the cam blank) considering $\Delta\gamma_X$ and $\Delta\gamma_Y$ is as follows:

$$\boldsymbol{r}_R=\begin{bmatrix}X_R\\Y_R\\Z_R\end{bmatrix}=\begin{bmatrix}\cos(\Delta\gamma_Y)&0&-\sin(\Delta\gamma_Y)\\0&1&0\\\sin(\Delta\gamma_Y)&0&\cos(\Delta\gamma_Y)\end{bmatrix}\cdot\begin{bmatrix}1&0&0\\0&\cos(\Delta\gamma_X)&\sin(\Delta\gamma_X)\\0&-\sin(\Delta\gamma_X)&\cos(\Delta\gamma_X)\end{bmatrix}\boldsymbol{r}_S$$
$$=\begin{bmatrix}\begin{gathered}[-(\Delta y\sin(\Delta\delta_X)+b\cos(\Delta\delta_X))\cos(\beta+\Delta\beta)+a\\+\Delta a+\Delta x\sin(\beta+\Delta\beta)]\cos(\Delta\gamma_Y)-\{(\Delta y\cos(\Delta\delta_X)\\-b\sin(\Delta\delta_X))\sin(\Delta\gamma_X)+[\Delta x\cos(\beta+\Delta\beta)\\+(\Delta y\sin(\Delta\delta_X)+b\cos(\Delta\delta_X))\sin(\beta+\Delta\beta)]\\\cdot\cos(\Delta\gamma_X)\}\sin(\Delta\gamma_Y)\end{gathered}\\ \\ \begin{gathered}-(\Delta y\cos(\Delta\delta_X)-b\sin(\Delta\delta_X))\cos(\Delta\gamma_X)\\+[(\Delta y\sin(\Delta\delta_X)+b\cos(\Delta\delta_X))\sin(\beta+\Delta\beta)\\+\Delta x\cos(\beta+\Delta\beta)]\sin(\Delta\gamma_X)\end{gathered}\\ \\ \begin{gathered}[-(\Delta y\sin(\Delta\delta_X)+b\cos(\Delta\delta_X))\cos(\beta+\Delta\beta)+a\\+\Delta a+\Delta x\sin(\beta+\Delta\beta)]\sin(\Delta\gamma_Y)+\{(\Delta y\cos(\Delta\delta_X)\\-b\sin(\Delta\delta_X))\sin(\Delta\gamma_X)+[\Delta x\cos(\beta+\Delta\beta)\\+(\Delta y\sin(\Delta\delta_X)+b\cos(\Delta\delta_X))\sin(\beta+\Delta\beta)]\\\cdot\cos(\Delta\gamma_X)\}\cos(\Delta\gamma_Y)\end{gathered}\end{bmatrix}\tag{3}$$

The manufactured pitch surface $\boldsymbol{r}_P$ of the globoidal cam can be obtained by transforming $\boldsymbol{r}_R$ to the coordinate system $O_CX_CY_CZ_C$ (fixed to the machined globoidal cam):

$$\boldsymbol{r}_P=\begin{bmatrix}\cos(\alpha+\Delta\alpha)&\sin(\alpha+\Delta\alpha)&0\\-\sin(\alpha+\Delta\alpha)&\cos(\alpha+\Delta\alpha)&0\\0&0&1\end{bmatrix}\boldsymbol{r}_R\tag{4}$$

The unit normal vector of $\boldsymbol{r}_P$ can be yielded as:

$$\boldsymbol{n}_P=\frac{\dfrac{\partial\boldsymbol{r}_P}{\partial\alpha}\times\dfrac{\partial\boldsymbol{r}_P}{\partial b}}{\left|\dfrac{\partial\boldsymbol{r}_P}{\partial\alpha}\times\dfrac{\partial\boldsymbol{r}_P}{\partial b}\right|}\tag{5}$$

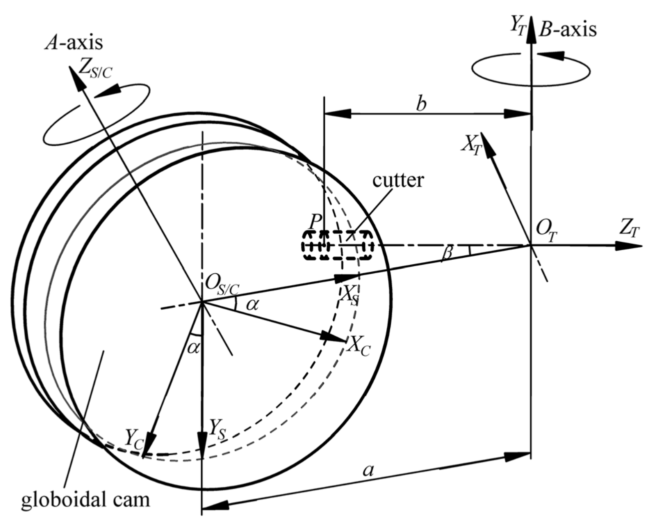

Fig. 4 Coordinate systems of the globoidal cam mechanism

where

$$\frac{\partial \boldsymbol{r}_S}{\partial \alpha}=\begin{bmatrix}\frac{\partial X_S}{\partial \alpha}\\ \frac{\partial Y_S}{\partial \alpha}\\ \frac{\partial Z_S}{\partial \alpha}\end{bmatrix}=\begin{bmatrix}-\beta(-\Delta y\sin(\Delta\delta_X)-b\cos(\Delta\delta_X))\\ \cdot\sin(\beta+\Delta\beta)+\Delta x\beta\cos(\beta+\Delta\beta)\\ 0\\ -\beta(-\Delta y\sin(\Delta\delta_X)-b\cos(\Delta\delta_X))\\ \cdot\cos(\beta+\Delta\beta)-\Delta x\beta\sin(\beta+\Delta\beta)\end{bmatrix} \quad (6)$$

$$\frac{\partial \boldsymbol{r}_R}{\partial \alpha}=\begin{bmatrix}\frac{\partial X_R}{\partial \alpha}\\ \frac{\partial Y_R}{\partial \alpha}\\ \frac{\partial Z_R}{\partial \alpha}\end{bmatrix}=\begin{bmatrix}\frac{\partial X_S}{\partial \alpha}\cos(\Delta\gamma_Y)-\frac{\partial Z_S}{\partial \alpha}\cos(\Delta\gamma_X)\sin(\Delta\gamma_Y)\\ \frac{\partial Z_S}{\partial \alpha}\sin(\Delta\gamma_X)\\ \frac{\partial X_S}{\partial \alpha}\sin(\Delta\gamma_Y)+\frac{\partial Z_S}{\partial \alpha}\cos(\Delta\gamma_X)\cos(\Delta\gamma_Y)\end{bmatrix} \quad (7)$$

$$\frac{\partial \boldsymbol{r}_P}{\partial \alpha}=\begin{bmatrix}\frac{\partial X_R}{\partial \alpha}\cos(\alpha+\Delta\alpha)-X_R\sin(\alpha+\Delta\alpha)\\ +\frac{\partial Y_R}{\partial \alpha}\sin(\alpha+\Delta\alpha)+Y_R\cos(\alpha+\Delta\alpha)\\ -\frac{\partial X_R}{\partial \alpha}\sin(\alpha+\Delta\alpha)-X_R\cos(\alpha+\Delta\alpha)\\ +\frac{\partial Y_R}{\partial \alpha}\cos(\alpha+\Delta\alpha)-Y_R\sin(\alpha+\Delta\alpha)\\ \frac{\partial Z_R}{\partial \alpha}\end{bmatrix} \quad (8)$$

$$\frac{\partial \boldsymbol{r}_R}{\partial b}=\begin{bmatrix}\frac{\partial X_R}{\partial b} & \frac{\partial Y_R}{\partial b} & \frac{\partial Z_R}{\partial b}\end{bmatrix}^T =\begin{bmatrix}\sin(\Delta\delta_X)\sin(\Delta\gamma_X)\sin(\Delta\gamma_Y)\\ -\cos(\Delta\delta_X)\sin(\beta+\Delta\beta)\cos(\Delta\gamma_X)\sin(\Delta\gamma_Y)\\ -\cos(\Delta\delta_X)\cos(\beta+\Delta\beta)\cos(\Delta\gamma_Y)\\ \\ \sin(\Delta\delta_X)\cos(\Delta\gamma_X)\\ +\cos(\Delta\delta_X)\sin(\beta+\Delta\beta)\sin(\Delta\gamma_X)\\ \\ -\sin(\Delta\delta_X)\sin(\Delta\gamma_X)\cos(\Delta\gamma_Y)\\ +\cos(\Delta\delta_X)\sin(\beta+\Delta\beta)\cos(\Delta\gamma_X)\cos(\Delta\gamma_Y)\\ -\cos(\Delta\delta_X)\cos(\beta+\Delta\beta)\sin(\Delta\gamma_Y)\end{bmatrix} \quad (9)$$

$$\frac{\partial \boldsymbol{r}_P}{\partial b}=\begin{bmatrix}\frac{\partial X_R}{\partial b}\cos(\alpha+\Delta\alpha)+\frac{\partial Y_R}{\partial b}\sin(\alpha+\Delta\alpha)\\ -\frac{\partial X_R}{\partial b}\sin(\alpha+\Delta\alpha)+\frac{\partial Y_R}{\partial b}\cos(\alpha+\Delta\alpha)\\ \frac{\partial Z_R}{\partial b}\end{bmatrix} \quad (10)$$

The surface of the machined globoidal cam $\boldsymbol{r}_C$ can be obtained by offsetting the pitch surface $\boldsymbol{r}_P$ with the distance equal to the roller radius r:

$$\boldsymbol{r}_C=\boldsymbol{r}_P\pm r\boldsymbol{n}_P \quad (11)$$

The ± sign in Eq. (11) is the result of the two side surfaces of the groove of globoidal cams.

3 Required models

3.1 Tolerance analysis

Combined with the machined globoidal cam surface derived in Section 2, the final surface deviation $f(\boldsymbol{X})$ of the machined globoidal cam can be described as the projection of the deviation vector of the cam surface on the direction of the surface normal vector $\boldsymbol{n}_N$:

$$f(\boldsymbol{X})=(\boldsymbol{r}_C-\boldsymbol{r}_N)\cdot\boldsymbol{n}_N \quad (12)$$

where $\boldsymbol{r}_C$ and $\boldsymbol{r}_N$ represent the machined globoidal cam surface (with deviation) and the theoretical globoidal cam surface (without deviation), respectively. Vector $\boldsymbol{X}$ is the deviation vector of the machine tool, and $\boldsymbol{X}=(x_1, x_2, \ldots, x_n)=(\Delta\alpha, \Delta\beta, \Delta\delta_X, \Delta\gamma_X, \Delta\gamma_Y, \Delta x, \Delta y, \Delta a)$. Thus, $\boldsymbol{r}_C$ is equal to $\boldsymbol{r}_N$ when the deviation vector $\boldsymbol{X}=\boldsymbol{0}$. Vector $\boldsymbol{n}_N$ is the unit normal vector of theoretical cam surface $\boldsymbol{r}_N$.

In order to predict deviation of final product (machined surface deviation), the first two terms of Taylor series of $f(\boldsymbol{X})$ in Eq. (12) at $\boldsymbol{X}_0=\boldsymbol{0}$ can be written as:

$$f(\boldsymbol{X})\approx f(\boldsymbol{X}_0)+\sum_{i=1}^{n}\left(\frac{\partial f}{\partial x_i}\right)\cdot x_i \ , \ \boldsymbol{X}=(x_1,x_2,\ldots,x_n) \quad (13)$$

where $(\partial f/\partial x_i)$ is the partial derivative of $f(\boldsymbol{X})$ with respect to x_i at $\boldsymbol{X}_0=\boldsymbol{0}$. As mentioned above, the machined surface deviation $f(\boldsymbol{X}_0)=0$ when deviation vector $\boldsymbol{X}_0$ of the machine tool is equal to $\boldsymbol{0}$.

The partial derivative $(\partial f/\partial x_i)$ is called the sensitivity coefficient, which represents the influence of the unit deviation of the i-th machine tool error on the final product deviation. The quantity $(\partial f/\partial x_i)\cdot x_i$ is the machined surface deviation caused by the i-th machine tool error. The sensitivity coefficient in Eq. (13) is commonly adopted for the calculation of the accumulated deviation of the final product, especially when the formulation of the final product deviation is very complicated. The sensitivity coefficients provide a convenient and accurate way for the analysis of the effect of incoming element deviation on output or final product deviation.

The worst-case (WC) model and the root sum square (RSS) model are two main models for tolerance analysis. The worst-case tolerance analysis considers the situation that all the component errors reach their extreme limits simultaneously. That is,

$$f_{wor}=\sum_{i=1}^{n}\left|\frac{\partial f}{\partial x_i}\right|\cdot|x_i| \quad (14)$$

The RSS method is the statistical method for tolerance analysis and is adopted under the normal distribution condition. The RSS method can be defined as follows:

$$f_{rss} = \sqrt{\sum_{i=1}^{n} \left(\frac{\partial f}{\partial x_i}\right)^2 x_i^2} \tag{15}$$

The RSS method is based on the condition that the possibility of reaching extreme deviation limits of all elements simultaneously is very small. Thus, the tolerance results by applying RSS method are usually larger than that by applying WC method.

3.2 Manufacture easiness index

Tolerance allocation is the process of determining allowable deviations in parts, components, and processes in order to meet final product quality or cost targets [28]. Reciprocal and exponential cost-tolerance models are popular used to build the objective function for tolerance synthesis. However, as mentioned above, the empirical data for the cost-tolerance models are insufficient and difficult to obtain. Thus, another criterion for tolerance allocation needs to be established.

Manufacture easiness index *EI*, which represents the level of manufacturing easiness or difficulty to achieve the target quality (tolerance), is applied to design optimal tolerance for the special machine tool. It is known that the easier the manufacture, the lower the cost. Thus, *EI* can also indirectly imply the manufacturing cost.

Generally speaking, it is more convenient to operate with unitless values when performing the manufacture easiness index. The mathematical model of normalized manufacture easiness index of the *i*-th element can be written as:

$$EI_i = \frac{|x_i| - |x_{i,\min}|}{|x_{i,\max}| - |x_{i,\min}|}, \quad |x_{i,\min}| \le |x_i| \le |x_{i,\max}|, \ \ i = 1, \ldots, n \tag{16}$$

where x_i is the real deviation of the *i*-th element, and $|x_{i,\min}|$ and $|x_{i,\max}|$ are the minimum and maximum tolerance restrictions of x_i.

According to Eq. (16), wide tolerance $|x_i|$ will increase the manufacture easiness, thus reducing the manufacture costs. If the tolerance $|x_i|$ reaches its maximum tolerance restriction $|x_{i,\max}|$, the manufacture easiness index EI_i of the *i*-th element is equal to 1. On the opposite, if the tolerance $|x_i|$ reaches its minimum tolerance restriction $|x_{i,\min}|$, EI_i is equal to 0. Henceforth, EI_i ranges from 0 to 1.

Then, the manufacture easiness *EI* of the final product can be yielded as:

$$EI = \sum_{i=1}^{n} \lambda_i \cdot EI_i \ , \sum_{i=1}^{n} \lambda_i = 1 \ , \ 0 < \lambda_i < 1 \tag{17}$$

where λ_i is the weight coefficient specified to the manufacture easiness EI_i of the *i*-th element.

In practice, the contributions of equivalent individual manufacture easiness EI_i to the final manufacture easiness *EI* are different, and λ_i is specified by quantifying the relative level of difficulty in manufacturing the qualified *i*-th element. Taken the special machine tool in Section 2 as an example, the restrictions of the squareness tolerance $\Delta\gamma_X$ is $0.005° \le |\Delta\gamma_X| \le 0.020°$, and the restrictions of the center distance error Δa is $0.002\ \text{mm} \le \Delta a \le 0.020$ mm. Thus, the individual manufacture easiness EI_i for achieving the accuracy $\Delta\gamma_X = 0.01°$ is the same as that for achieving the accuracy $\Delta a = 0.008$ mm, while the two manufacture easiness have different effects on the final manufacture easiness of the machine tool. It is known from the industrial engineers, the accuracy of $\Delta\gamma_X$ is more difficult to achieve than Δa. Henceforth, a larger weight coefficient is specified to $\Delta\gamma_X$. It means that a small increase of EI_i of $\Delta\gamma_X$ can improve total manufacture easiness *EI* a lot. In the following optimal tolerance design, the maximum *EI* will serve as the objective for the tolerance allocation. Thus, the larger the weight coefficient of $\Delta\gamma_X$, the larger the tolerance of $\Delta\gamma_X$ can be obtained, and then the total manufacture easiness will be improved.

Generally speaking, the tolerance-cost-optimization is widely used for optimal tolerance design. The optimal tolerances are essentially affected by the tolerance-cost relationship. However, it is not available to obtain sufficient empirical data, for the reason that the special machine tool discussed in this paper is a new design. In addition, hardly any published literatures deal with the tolerance-cost relation. Based on the reasons above, we established a new optimal criterion, manufacture easiness index *EI*, which can evaluate not only the manufacture easiness but also manufacture costs. The manufacture easiness model is very suitable for the tolerance design of new product. All the coefficients we needed in the *EI* model should be provided by the experienced industrial engineers.

3.3 Optimization model for tolerance allocation

The optimization model for tolerance allocation is formulated to maximize the manufacture easiness subject to final product quality and the manufacture constrains or restrictions. It has been concluded by Prabhaharan that if cost is not the important factor to the company but the precision is the crucial factor then the tolerances may be allotted by worst-case analysis, or if the cost is important but the quality is less important, then it is better to allocate tolerances using the root sum square method [29].

The optimal tolerance results can be obtained by solving the following optimization problem

$$\begin{aligned}&\max\ EI(\boldsymbol{t})\\&\text{subject to}\ f(\boldsymbol{t})\le C_0\\&\qquad t_{i,\min}\le t_i\le t_{i,\max}\quad ,i=1,2,\ldots,n\end{aligned} \tag{18}$$

where $\boldsymbol{t}(t_1, t_2,\ldots, t_n)$ is the tolerance vector which contains all the element tolerances to be taken into account. The objective $EI(\boldsymbol{t})$ can be determined by applying Eqs. (16) and (17). $f(\boldsymbol{t})$ is the accumulated deviation of final product caused by $\boldsymbol{t}$. The constraint $f(\boldsymbol{t})\le C_0$ ensures the final product deviation will meet the requirement C_0. The WC model or the RSS model explained in Eq. (14) or Eq. (15) can be used for tolerance accumulation. $t_{i,\min}$ and $t_{i,\max}$ are the lower and upper design specification limits of t_i, respectively.

4 Application examples

A special machine tool for manufacturing globoidal cams is applied to demonstrate the practicality and validity of the proposed approach. As shown in Fig. 5, a globoidal cam is being machined by this special machine tool. The globoidal cam is mounted on the power supporter, and the position of the power supporter along the *W*-axis is fixed when the center distance a is determined. The position of the cutting tool along the *Z*-axis is determined by b. In the machining processes, the globoidal cam rotates around the *A*-axis and swivels around the *B*-axis to simulate the respective relative relationship between the globoidal cam and the follower roller (see Fig. 1). This globoidal cam is used in Automatic Tool Changer (ATC) of CNC machines. The basic parameters of this type of globoidal cam are as follows: $a=160$ mm, 37.5 mm$\le b$

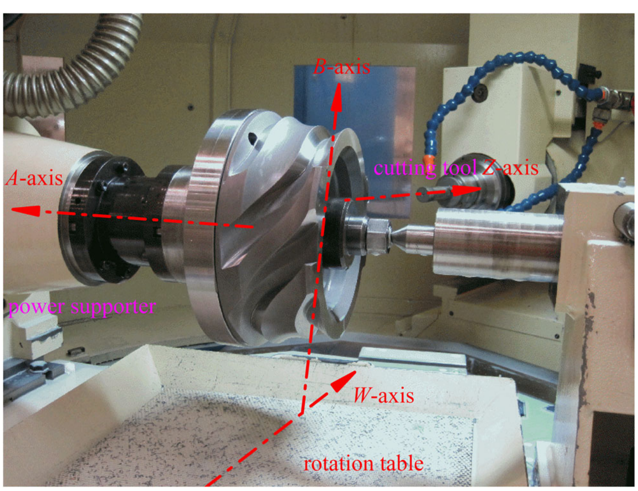

Fig. 5 Machining picture of the special machine tool

Table 2 Motion sequences and motion curves of ATC

α(deg)	β (deg)	Motion	Motion curves
0–2	0	Dwell	Dwell
2–52	0–90	Catching cutters	MS
52–122.5	90	Disengaging cutters	Dwell
122.5–237.5	90–270	Exchanging cutters	MS
237.5–308	270	Inserting cutters	Dwell
308–358	270–180	Releasing cutters	MS
358–360	180	Dwell	Dwell

$\le$54.5 mm, $r=13$ mm, and the diameter of the cam d is 265 mm. The motion sequences and motion curves which determine the machined cam surface is shown in Table 2.

In order to get a comprehensive understanding of tolerance allocation for the special machine tool, the mapping of grooves of this type of globoidal cam is simulated in Fig. 6. It can be seen that 4 tool paths are needed for machining the globoidal cam. When machining, the cutting tool follows the motion along every tool path. As shown in Fig. 6, the machining of no. 3 tool path begins from position *A*, then crosses the 360° position of α. As the globoidal cam is a torus surface, positions 0° and 360° are the same. Thus, the no. 3 tool path is the longest path, which begins from *A* position, then crosses 360°(0°), and ends at *B* position.

4.1 Results for tolerance analysis

As illustrated in Table 1, the set of machine tool errors contains 8 incoming element tolerances, including $\Delta\alpha$, $\Delta\beta$, $\Delta\delta_X$, $\Delta\gamma_X$, $\Delta\gamma_Y$, Δx, Δy, and Δa. According to the practice outlined in Section 3, the sensitivity coefficients of the 8 element tolerances are obtained by substituting Eqs. (1)–(12) to Eq. (13). By applying the VS software, the sensitivity coefficients of angular elements and displacement elements corresponding to no. 3 tool path are shown in Figs. 7 and 8, respectively.

According to Eqs. (12) and (13), the sensitivity is positive when the deviation of cam surface is toward $+\boldsymbol{n}_N$ direction and vice versa. A larger absolute value of sensitivity coefficient means a greater effect on the cam surface deviation. As can be seen in Fig. 7, the values of the sensitivities in descending order with respect to five angular tolerances are $\Delta\alpha$ followed by $\Delta\beta$ followed by $\Delta\gamma_Y$ followed by $\Delta\delta_X$ and then followed by $\Delta\gamma_X$.

In the dwell period, during the domain of the cam rotation angle (52°, 122.5°) and (237.5°, 308°), the absolute value of sensitivity coefficient with respect to $\Delta\beta$ and $\Delta\gamma_Y$ are relatively large. Thus, the machined cam surface is sensitive to $\Delta\beta$ and $\Delta\gamma_Y$. According to the machining principle described in Section 2.1, the rotation angle error of *B*-axis $\Delta\beta$ is equivalent to the turret angle deviation. Thus, it would not be difficult to

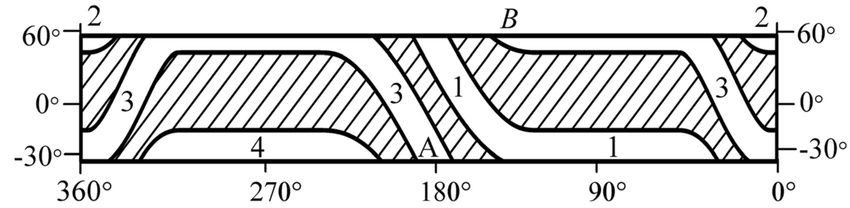

Fig. 6 The mapping of grooves of the globoidal cam

understand $\Delta\beta$ would have a great effect on the cam surface deviation. Furthermore, from the configuration of the machine tool shown in Fig. 3, $\Delta\gamma_Y$ will also cause the turret angle error indirectly. As explained in Table 2, the turret angle deviation in the dwell period determines the positioning accuracy of the exchange cutter manipulator. Henceforth, $\Delta\beta$ and $\Delta\gamma_Y$ have great effect on the tool exchange accuracy of ATC.

In the indexing period, $\Delta\alpha$ has a great effect on the surface deviation of the machined globoidal cam. In addition, the variation trends of sensitivity coefficients with respect to $\Delta\alpha$ and $\Delta\delta_X$ are nearly consistent. Thus, it may cause the superposition effect on the machined surface deviation. Henceforth, the deviation of them should be strictly controlled. Other errors $\Delta\beta$ and $\Delta\gamma_Y$ should be given enough attention, for their sensitivity coefficients are relatively large in whole cycle of cam operation. The effect of the squareness error $\Delta\gamma_X$ on the machined surface deviation is the smallest among the five angular deviations. In practice, the tolerance of $\Delta\gamma_X$ can be specified a bit larger.

The sensitivities of the displacement deviations including Δx, Δy, and Δa are shown in Fig. 8. The results show that the deviation of Δx has a great effect on the machined cam surface. Especially in the dwell period, Δx will transmit equivalent deviation to the machined cam surface. Thus, the accuracy of Δx should be paid much attention. Although the error Δy has no effect on the machined surface deviation in the dwell period, the variation trends of Δx and Δy are nearly the same in the indexing period. Thus, the two errors should be strictly controlled to avoid the appearance of their superposition effect on the surface deviation. In the dwell period, the sensitivity coefficients of Δx and Δa are more than 0.85. Thus, the narrow tolerances should be specified to Δx and Δa from the consideration of tool exchange accuracy of cutter manipulator.

4.2 Results for tolerance allocation

As the practice outlined in Section 3.3, the optimization model for optimal tolerance allocation is established. The objective function, manufacture easiness index *EI*, is expressed in Eqs. (16) and (17). The requirement of the final quality C_0 of the machined globoidal cam surface is 0.03 mm. Since the precision of the special machine tool is more important than the cost, the worst-case (WC) method in Eq. (14) is used for tolerance accumulation. Substituted Eq. (14) into Eq. (18), the constraints of the final quality of the globoidal cam is obtained. The optimization problems in Eq. (18) are solved by using linear programming of MATLAB Optimization Toolbox. The lower and upper design specification limits, the weight coefficients for the 8 elements, and the optimal tolerance results are listed in Table 3.

Larger weight coefficient λ_i implies a higher level of manufacturing difficulty or higher cost. Therefore, in the optimization process, the manufacture easiness can be increased

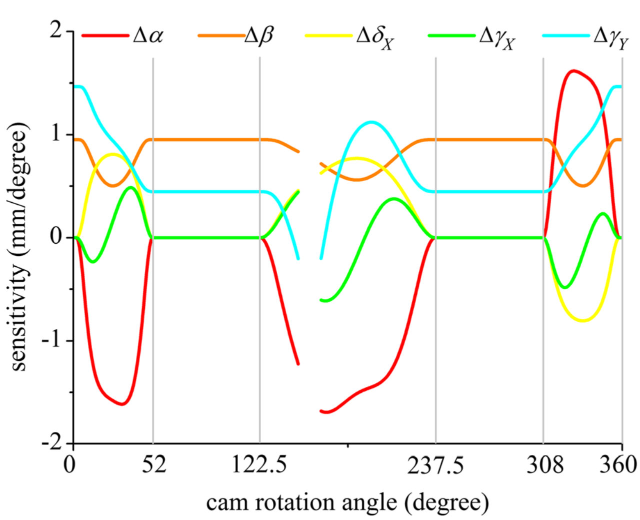

Fig. 7 Sensitivities of angular elements

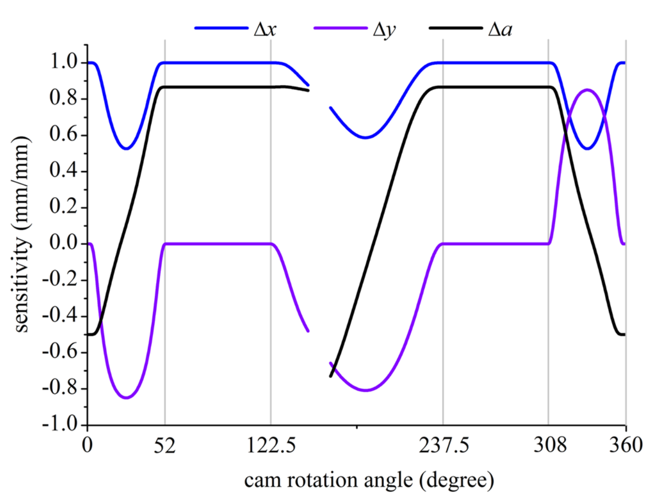

Fig. 8 Sensitivities of displacement elements

Table 3 Results for optimal tolerance allocation

t	Constraints		λ_i	Results
	Lower	Upper		
$\Delta\alpha$ (deg)	0.001	0.005	0.125	0.0050
$\Delta\beta$ (deg)	0.001	0.005	0.125	0.0050
$\Delta\delta_X$ (deg)	0.005	0.020	0.150	0.0050
$\Delta\gamma_X$ (deg)	0.005	0.020	0.150	0.0119
$\Delta\gamma_Y$ (deg)	0.005	0.020	0.150	0.0080
Δx (mm)	0.002	0.020	0.100	0.0020
Δy (mm)	0.002	0.020	0.100	0.0020
Δa (mm)	0.002	0.020	0.100	0.0020

through enlarging its tolerance t_i. The weight coefficient of $\Delta\gamma_X$ is one of the largest ones (see Table 3), but its sensitivity is relatively small among the angular tolerances (see Fig. 7). It means that the accuracy of $\Delta\gamma_X$ is difficult to achieve but it has a relatively small effect on the surface error. Thus, the tolerance of $\Delta\gamma_X$ can be enlarged to increase the manufacture easiness. Therefore, we can observe from the results of Table 3 that $\Delta\gamma_X$ is the largest among the five angular deviations. It is shown in Table 3, the weight coefficient λ_i of $\Delta\gamma_Y$ is equal to that of $\Delta\gamma_X$ and is also the largest one. It will also increase the manufacture easiness *EI* significantly by enlarging $\Delta\gamma_Y$. However, as shown in Fig. 7, the sensitivity coefficient of $\Delta\gamma_Y$ is larger than that of $\Delta\gamma_X$; thus, it has greater effect on the machined surface error than $\Delta\gamma_X$. It is the reason why a narrower tolerance is specified to $\Delta\gamma_Y$ compared with $\Delta\gamma_X$. For the displacement elements in Table 3, we see that Δx, Δy, and Δa reached their minimum design limits, because their accuracy is easy to achieve, and their influence on the cam surface deviation is relatively large.

The optimal tolerance results are used as the guideline for manufacturing the special machine tool which is shown in Fig. 9. As the special machine tool is a new design, the tolerances of the axes and their relative positions of the machine tool should be reasonably designed before manufacture. The industrial engineers have designed the tolerances by using the tolerance allocation results in Table 3 for reference. The final tolerances of the special machine tool designed by engineers are as follows: $\Delta\alpha = 0.003°$, $\Delta\beta = 0.003°$, $\Delta\delta_X = 0.005°$, $\Delta\gamma_X = 0.008°$, $\Delta\gamma_Y = 0.008°$, $\Delta x = 0.002$ mm, $\Delta y = 0.002$ mm, $\Delta a = 0.002$ mm.

4.3 Experimental results

The special machine tool for manufacturing globoidal cams is designed and manufactured (see Fig. 9) by taking the optimal tolerance results (see Table 3) as a reference. In order to validate the synthesis results, a globoidal cam machined by this special machine tool is tested. The measurement is performed on a CMM with measurement uncertainty of $\mathrm{MPE_E}(\mu\mathrm{m}) = 2.5 + 3.3\,L/1000$ (see Fig. 10).

The green one in Fig. 10 is the theoretical model of the globodal cam. The machined globoidal cam can be measured by choosing several points on the theoretical model. The measured results of the no. 3 groove (corresponding to no. 3 groove in Fig. 6) are listed in Table 4.

The theoretical points of the globoidal cam surface are given by X, Y, and Z. The measured deviations of the machined cam surface in three directions are noted as ΔX, ΔY, and ΔZ. The measured surface deviation is noted by ΔE and is defined by the root sum squares of ΔX, ΔY and ΔZ.

It can be seen from the listed results in Table 4, the measured surface deviation is smaller than the final quality requirement $C_0 = 0.03$ mm. It confirms the effectiveness of the proposed approach. Furthermore, the surface deviation in the dwell period is smaller than that in the indexing period. That may be the reason that the deformation happened in the machining processes.

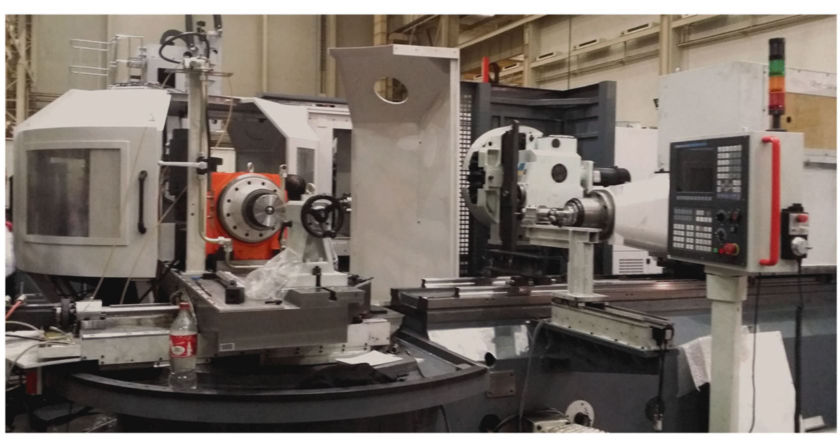

Fig. 9 The special machine tool for manufacturing globoidal cams

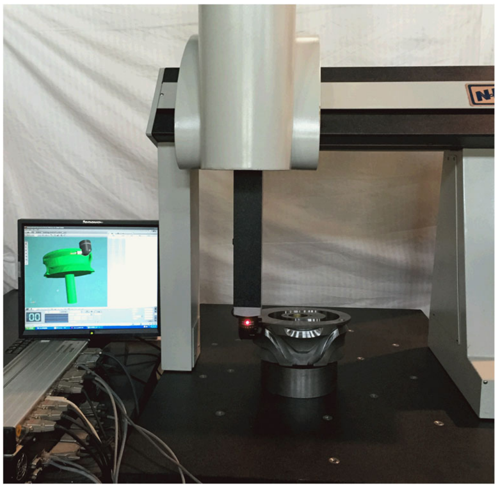

Fig. 10 Measurement of the machined globoidal cam surface

5 Conclusions

Many engineers in machine tool plants faced with the problem of how to determine the optimal tolerance of machine tools. This paper presents a simple yet comprehensive approach for optimal tolerance allocation of the special machine tool for manufacturing globoidal cams. The influence of machine tool errors on the surface deviation of the machined globoidal cam is also studied. The conclusions are summarized as follows:

1. Based on the conjugate theory and differential geometry, the expression for the machined surface of globoidal cam by considering two rotary errors, three squareness errors, and three linear offset errors is identified.

2. The sensitivity coefficients of machine tool errors to the cam surface deviation are calculated with the help of the VS software. Compared with the five angular errors, the machined cam surface in the dwell period is sensitive to $\Delta\beta$ and $\Delta\gamma_Y$. The rotational angle error $\Delta\alpha$ has a great effect on the machined cam surface in indexing period. The variation trends of $\Delta\alpha$ and $\Delta\delta_X$ are nearly consistent. Thus, the deviation of them should be strictly controlled. The linear offset error Δx of spindle in the direction which is in the horizontal plane and perpendicular to the spindle has the greatest effect on the machined cam surface among the three linear errors.

3. By applying the manufacture easiness index as the objective, the optimization model is built subjected to final quality of machined cam surface and the manufacture constraints or restrictions. The WC method is used to formulate the accumulated error of cam surface caused by machined tool errors. The MATLAB Optimization Toolbox is utilized to solve the optimization model.

4. The optimization results are used as a guideline for designing and manufacturing the special machine tool. A globoidal cam machined by this machine tool is measured on a CMM. The measured results meet the final quality requirements, which validate the proposed approach in this paper.

We expect the proposed approach can be applied to machine tool plants for CAD/CAM, since the calculation program has been accomplished based on the VS and MATLAB software. The further study can be extended to incorporate the thermal and dynamic errors of the special machine tool and the deformation of the cam surface in machining processes.

Table 4 The measured results for right surface of no. 3 groove

Theoretical value (mm)			Actual deviation (10^{-2} mm)			Error (10^{-2} mm)
X	Y	Z	ΔX	ΔY	ΔZ	ΔE
117.8534	37.8135	−27.0401	0.28	2.48	−1.34	2.83
119.6313	35.5783	−28.3736	0.43	2.19	−1.40	2.63
121.3465	32.9146	−29.7810	−0.37	2.14	−0.8	2.31
123.1076	30.6341	−30.6553	−0.94	0.85	−0.45	1.34
123.2212	30.2546	−30.8441	−0.99	1.60	−0.28	1.90
123.5407	29.5492	−31.1434	−0.39	2.09	0.08	2.13
124.7698	28.2216	−31.4081	−0.67	1.34	0.23	1.52
126.0000	25.9906	−32.0269	−0.54	1.47	1.11	1.92
127.2220	23.8065	−32.4490	−1.81	1.95	1.13	2.89
123.2940	−28.5592	−31.8112	−1.47	0.60	2.52	2.98

Acknowledgments This research was funded by the National Science and Technology Major Project, China, under contract 2013ZX04008-021. The authors would like to acknowledge the support and contribution from the Beijing No. 1 Machine Tool Plant for their help with manufacturing and be grateful to the Key Lab of Mechanical Engineering, Beijing University of Technology, China.

References

1. Yan HS, Chen HH (1996) Geometry design of globoidal cams with generalized meshing turret-rollers. ASME J Mech Des 118:243–249
2. Backhouse CJ, Jones JR (1990) Envelope theory applied to globoidal cam surface geometry. Proc Inst Mech Eng Part C-J Eng Mech Eng Sci 204:409–416
3. Ji S, Zhao J, Zhang Y (2015) An application of geodesics to the calculation of the rib-thickness of globoidal cam mechanisms. Mech Mach Theory 87:163–176
4. Tsay DM, Ho HC (2001) Consideration of manufacturing parameters in the design of grooved globoidal cam indexing mechanisms. Proc Inst Mech Eng Part C–J Eng Mech Eng Sci 215:95–103
5. Cheng HY (2002) Optimum tolerances for globoidal cam mechanisms. JSME Int J Ser C Mech Syst Mach Elem Manuf 45(2):519–526
6. Wang WH, Tseng CH, Tsay CB (1999) On the optimization of spatial cam mechanisms considering mechanical errors. Int J Model Simul 19(1):94–100
7. Chang WT, Wu L (2013) Tolerance analysis and synthesis of cam-modulated linkages. Math Comput Model 57(3–4):641–660

8. Geetha K, Ravindran D, Siva Kumar M, Islam MN (2015) Concurrent tolerance allocation and scheduling for complex assemblies. Robot Comput-Integr Manuf 35:84–95
9. Hsueh CC, Lin PD, Sasian J (2010) Worst-case-based methodology for tolerance analysis and tolerance allocation of optical systems. Appl Opt 49(31):6179–6188
10. Mansuy M, Giordano M, Hernandez P (2011) A new calculation method for the worst case tolerance analysis and synthesis in stack-type assemblies. Comput Aided Des 43:1118–1125
11. Zhu H, Zhou X, Li H (2015) A novel tolerance analysis for mechanical assemblies based on Convex Method and non-probabilistic set theory. Int J Adv Manuf Technol. doi:10.1007/s00170-015-7634-9
12. Schleich B, Wartzack S (2015) Evaluation of geometric tolerances and generation of variational part representatives for tolerance analysis. Int J Adv Manuf Technol 79:959–983
13. Creveling CM (1997) Tolerance design: a handbook for developing optimal specifications. Addison-Wesley, Boston, pp 124–148
14. Gaurav A (2006) Statistical tolerance analysis and allocation for assemblies using tolerance-maps. Dissertation, Arizona State University
15. Chase KM (1991) A survey of research in the application of tolerance analysis to the design of mechanical assemblies. Res Eng Des 3:23–37
16. Nigam SD, Turner JU (1995) Review of statistical approaches to tolerance analysis. Comput Aided Des 27:6–15
17. Hong YS, Chang TC (2002) A comprehensive review of tolerancing research. Int J Prod Res 40(11):2425–2459
18. Singh PK, Jain PK, Jain SC (2009) Important issues in tolerance design of mechanical assemblies. Part 1: tolerance analysis. Proc Inst Mech Eng Part B-J Eng Manuf 223:1225–1247
19. Govindaluri MS, Shin S, Cho BR (2004) Tolerance optimization using the Lambert W function: an empirical approach. Int J Prod Res 42(16):3235–3251
20. Spotts MF (1973) Allocation of tolerances to minimize cost of assembly. ASME J Eng Ind 95:762–764
21. AL-Ansary MD, Deiab IM (1997) Concurrent optimization of design and machining tolerances using the genetic algorithms method. Int J Mach Tools Manuf 37(12):1721–1731
22. Lee WJ, Woo TC, Chou SY (1993) Tolerance synthesis for nonlinear systems based on nonlinear programming. IIE Trans 25(1):51–61
23. Sfantsikopoulos MM (1990) A cost-tolerance analytical approach for design and manufacturing. Int J Adv Manuf Technol 5:126–134
24. Yeo SH, Ngoi BKA, Poh LS, Hang C (1997) Cost-tolerance relationships for non-traditional machining processes. Int J Adv Manuf Technol 13:35–41
25. Zhang C, Wang HP (1998) Robust design of assembly and machining tolerance allocations. IIE Trans 30:17–29
26. Singh PK, Jain PK, Jain SC (2009) Important issues in tolerance design of mechanical assemblies. Part 2: tolerance synthesis. Proc Inst Mech Eng Part B-J Eng Manuf 223:1249–1287
27. Wang Y, Zhai WJ, Yang LP, Wu WG, Ji SP, Ma YL (2007) Study on the tolerance allocation optimization by fuzzy-set weight-center evaluation method. Int J Adv Manuf Technol 33:317–322
28. Li Z, Kokkolaras M, Papalambros P, Hu SJ (2008) Product and process tolerance allocation in multistation compliant assembly using analytical target cascading. ASME J Mech Des 130: 091701-1–091701-9
29. Prabhaharan G, Asokan P, Ramesh P, Rajendran S (2004) Genetic-algorithm-based optimal tolerance allocation using a least-cost model. Int J Adv Manuf Technol 24:647–660